Dimethyl Sulfide on Cu{111}: Molecular Self-Assembly and Submolecular Resolution Imaging

Stephen C. Jensen, Ashleigh E. Baber, Heather L. Tierney, and E. Charles H. Sykes*

Department of Chemistry, Tufts University, Medford, Massachusetts 02155-5813

ARTICLE

ABSTRACT The literature contains many studies of thiol-based, self-assembled monolayers (RSH); however, thioethers (RSR) have barely begun to be explored, despite having the potential advantages of being more resistant to oxidation and allowing for the control of self-assembly parallel to the surface. This paper describes a low-temperature scanning tunneling microscopy investigation of dimethyl sulfide on Cu{111}. Previous work on the adsorption of dibutyl sulfide on Cu{111} revealed that intermolecular van der Waals interactions directed the parallel ordering of dibutyl sulfide molecules in linear rows. Upon annealing to 120 K, small dibutyl sulfide domains reordered into very large, ordered domains free of defects. The current study reveals the effect of the shorter alkyl chain length of dimethyl sulfide on both the rate of diffusion and the packing structure of the molecule. At a medium surface coverage and at 78 K, it was found that dimethyl sulfide is mobile and forms large, ordered islands without the 120 K annealing that was required for dibutyl sulfide to arrange. Also, the molecular packing structure evolves from quadrupole—quadrupole interactions and results in a perpendicular arrangement of neighboring molecules instead of the parallel arrangement observed for dibutyl sulfide. We show high-resolution images of the dimethyl sulfide islands in which submolecular features are revealed. These high-resolution data allow us to propose a structural model for the adsorption site of each dimethyl sulfide molecule within the ordered structures. These results demonstrate that the length of the alkyl side chain is an important factor in determining how thioethers self-assemble on metal surfaces.

KEYWORDS: thioether · dimethyl sulfide · Cu{111} · STM · self-assembly

Self-assembled monolayers (SAMs) have been thoroughly investigated due to their utility in many fields such as sensing, device assembly, molecular electronics, and microelectromechanical systems.[1–13] Thiol (RSH) SAMs are by far the most extensively studied in the literature due to their robustness and the ability to control their assembly in the dimension perpendicular to the surface of the metal.[1,5,9,12,14] There are, however, problems with thiol SAMs because they contain structural defects like etch pits and rotational domain boundaries, which make them more susceptible to oxidation and displacement.[5,9,15] Most studies of thiol SAMs have been conducted on Au{111}, but as this paper is concerned with thioether adsorption on Cu{111}, we will also discuss the relevant literature about thiol self-assembly on Cu.[16–21] Theoretical and experimental studies have shown that, when thiol SAMs form on Cu{111}, they reconstruct the top layer of the Cu surface and create different types of ordered overlayer structures based on the surface coverage. Both methanethiolate and octanethiolate were investigated by Driver *et al.* on Cu{111}, and the STM data revealed that both molecules reconstructed the outermost Cu layers and ordered in either square or honeycomb structures, depending on the surface coverage.[17,21]

Thioethers (RSR) are similar to thiols but have two alkyl tails that cause them to lie parallel to the surface instead of arranging nearly perpendicular like thiols. This adsorption geometry allows for control over the packing density in the dimensions parallel to the surface by simply adjusting side-chain length. Thioether SAMs may also be preferable to thiol SAMs for many uses because they are more resistant to oxidation. Despite these advantages, there has only been very limited research conducted on the self-assembly of thioethers on metals.[22–27] Previous studies of long-chained thioethers on highly oriented pyrolytic graphite (HOPG) revealed that they arrange parallel to each other in rows held together by van der Waals forces.[28,29] Hara *et al.* investigated the adsorption characteristics of dioctadecyl sulfide on Au{111} and found that, unlike thiol adsorption, thioethers physisorb on the surface and do not lift the $22 \times \sqrt{3}$ reconstruction of Au.[23,24] In a recently published paper, we showed that, at 78 K, thioethers as small as dibutyl sulfide also arrange themselves in linear rows to form a SAM in which the ordering is driven by van der Waals forces between

*Address correspondence to charles.sykes@tufts.edu.

Received for review September 19, 2007 and accepted November 01, 2007.

Published online November 30, 2007.
10.1021/nn700243r CCC: $37.00

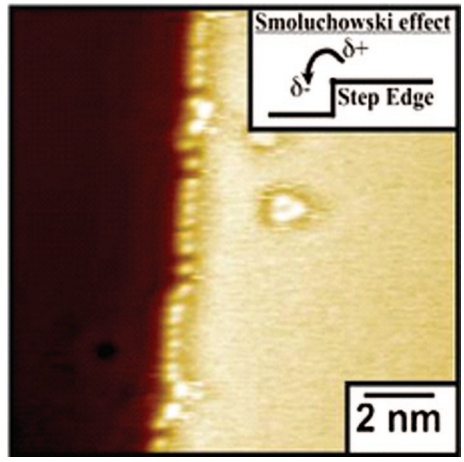

Figure 1. STM image of 0.03 ML (0.04 Langmuir (L)) of dimethyl sulfide on a Cu{111} surface at 78 K. The molecules adsorb preferentially at sites above the step edges and at defects. Image conditions: V_{tip} = 0.5 V, I = 0.10 nA.

the alkyl side chains.[30] Since sulfur is a relatively electronegative atom, it seems likely that shorter thioethers will have weaker intermolecular van der Waals forces, and quadrupole−quadrupole interactions between neighboring molecules will begin to dominate the packing energetics. In this paper we investigate the smallest thioether, dimethyl sulfide, in an effort to investigate the effect of a very short alkyl side chain on thioether self-assembly.

RESULTS AND DISCUSSION

Figure 1 shows a typical scanning tunneling microscopy (STM) image of Cu{111} with 0.03 monolayer (ML) of dimethyl sulfide deposited at 78 K. The molecules preferentially adsorb at substrate step edges due to the Smoluchowski effect, in which electron density is redistributed from the top of the step edge to the bottom.[31] This charge transfer creates a slight electropositive area on the top of the step edge and an electronegative area on the bottom of the step edge.

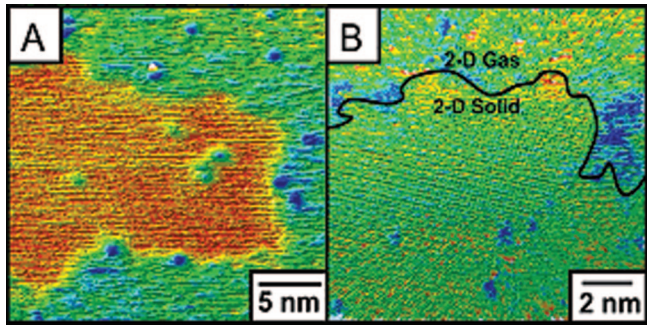

Figure 2. STM images of dimethyl sulfide islands on Cu{111} at 78 K: surface coverage of (A) 0.07 ML (0.09 L) and (B) 0.30 ML (0.36 L). In panel A, the dimethyl sulfide islands appear ~0.1 nm higher than the Cu{111} terrace. In panel B, the dimethyl sulfide island appears the same height as the Cu terrace. The gap conditions used in panel B move the tip closer to the surface, at which point it perturbs the molecules as it scans. This mobilizes dimethyl sulfide molecules on the bare Cu(111) terrace that then image the same height as the island. Image conditions: (A) V_{tip} = −0.25 V and I = 0.1 nA; (B) V_{tip} = −0.05 V and I = 0.5 nA.

The electronegative sulfur atom in the center of the dimethyl sulfide molecule binds more strongly to the top of the step edge. When dimethyl sulfide is deposited on the Cu{111} surface at 78 K, the molecules diffuse across the terraces and find preferential adsorption sites at the step edges.

In addition to step edges, small amounts of single missing atom defects are also present on the terraces of the Cu{111} surface. Like step edges, these defects also perturb the electron density by scattering the surface-state electrons and create standing waves.[32] When dimethyl sulfide is dosed on the surface, the molecules first adsorb at the step edges, but once the areas above the step edges are fully occupied, the molecules then adsorb at single atom defect sites on the terrace. A small cluster of three dimethyl sulfide molecules absorbed on such a defect on the Cu terrace is seen in Figure 1. Step edges represent much more of a perturbation to the electronic state of the surface than a single missing or impurity atom on a terrace. Therefore, steps represent the most stable adsorption site for dimethyl sulfide and are populated before terrace defects.

As more dimethyl sulfide is dosed on the surface, the molecules start to form ordered islands on the Cu{111} terrace. Figure 2A shows 0.07 ML of dimethyl sulfide, while Figure 2B has a surface coverage of 0.30 ML. As the coverage is increased, both the number and the size of the islands increase. These islands are well ordered and continuous and grow without formation of etch pits that are commonly present in thiol SAMs.

Figure 2B was recorded with a lower voltage and higher tunneling current than Figure 2A. These gap conditions decrease the tip–sample distance, increase the perturbation of the molecules by the tip, and have the effect of mobilizing molecules in the areas around the ordered island. These mobile molecules constantly leave and rejoin the island, but they move faster than the tip can image them and therefore appear as spikes in the image that have the same height as the molecules in the island. This effect leads to an image in which the island appears the same height as the surrounding Cu terrace.[33,34] We never observed scattering of the surface-state electrons from the islands of dimethyl sulfide, even though we imaged at a wide variety of tip biases between ±0.05 and ±1 V. This was most probably because the subtle contrast of standing waves was masked by mobile molecules on the surface.

Figure 3 shows submolecular resolution images of dimethyl sulfide within an ordered island. The only difference between panels A and B of Figure 3 is that there has been a change in the STM tip state. Both images were recorded with the same tunneling conditions, about 5 min apart, in exactly the same area of the surface. The tip state in Figure 3A is fine enough to resolve the two methyl groups of each molecule, and each mol-

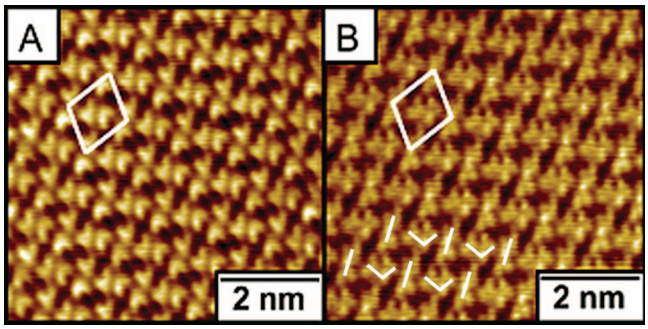

Figure 3. High-resolution STM images of the molecular packing structure of the dimethyl sulfide islands on Cu{111} at 78 K at a surface coverage of 0.3 ML (0.36 L). The unit cell is depicted with a white box. These two images are of exactly the same area of the surface; differences in their appearance are due to different tip states. Conditions for both images: $V_{tip} = -0.05$ V, $I = 1$ nA.

ecule looks like a "bowtie". There is one whole dimethyl sulfide molecule at the center of the unit cells, marked with white parallelograms, and a molecule at each vertex. Figure 3B shows an image with an even finer tip state than in Figure 3A, in which individual atoms within each molecule can be seen. By comparison of the two images, we conclude that the largest protrusion at the center of each molecule imaged in Figure 3B corresponds to the position of the S atom at the center of the molecule. Each of the methyl groups of the molecule appear in Figure 3B as two smaller protrusions. This complex shape may originate from the electron cloud surrounding the two upward-facing H atoms of the methyl groups. It is interesting to note from Figure 3B that the position of the sulfur group varies depending on the position of the molecule in the island. The molecules aligned nearly vertically (as highlighted by straight white lines in Figure 3) image with the S atom centralized along the molecular axis, whereas in the molecules lying nearly horizontally (as highlighted by bent white lines), the S atom appears offset. These two different molecular shapes suggest that the molecules are adsorbed on different surface sites. This point will be discussed later in the paper. The white parallelograms in Figure 3 show the unit cell of the packing structure. It is interesting to note that the scanning conditions used for Figure 3 are more perturbative than those that mobilized molecules at the edges of the islands in Figure 2b. However, scanning the center of a large island where the molecules are locked into place allowed us to image clearly without disturbing the molecules at the edges.

Both images in Figure 3 indicate that dimethyl sulfide packs in a perpendicular arrangement or, more technically, a herringbone packing structure.[35] This is a common packing structure adopted by quadrupolar molecules.[35,36] The inset of Figure 4 shows a schematic of a herringbone packing structure that allows for maximum electrostatic interaction between the electronegative S atoms and the electropositive methyl groups.

Figure 4 shows an area of the surface with a 0.3 ML (0.36 L) coverage of dimethyl sulfide. Two ordered islands, in which the packing structure is rotated by 60° to each other, are observed. STM imaging of large areas revealed that all of the dimethyl sulfide islands on the surface have this same three-fold symmetry. This fact gives us the first evidence that the packing structure is commensurate with the Cu substrate lattice. Detailed measurements of ordered arrays of dimethyl sulfide were taken and the lateral dimensions compared with the atomic positions of the underlying Cu{111} terrace in order to determine an overlayer structure. Figure 5A is a zoomed-in version of Figure 3B, and a proposed model of the structure is shown in Figure 5B. The proposed structure is a $(\sqrt{7} \times \sqrt{7})$R19.1° unit cell, as indicated by the black parallelograms in Figure 5. The

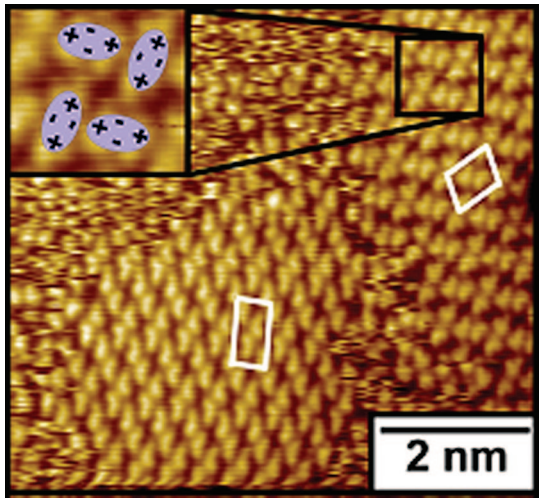

Figure 4. STM images of two dimethyl sulfide islands rotated 60° with respect to each other on Cu{111} at 78 K. White boxes are unit cells for both islands. The inset depicts the herringbone packing structure of the islands that maximizes quadrupole−quadrupole interactions between molecules. Image conditions: $V_{tip} = -0.05$ V, $I = 1$ nA.

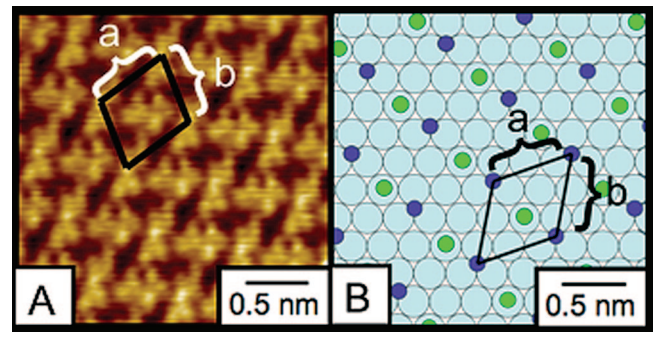

Figure 5. (A) Cropped image of dimethyl sulfide on Cu{111} at 78 K, taken from Figure 3B. (B) Proposed structural model for the molecular packing of dimethyl sulfide. The black parallelogram represents the $(\sqrt{7} \times \sqrt{7})$R19.1° unit cell. Light blue circles represent the Cu{111} lattice, dark blue circles correspond to the position of the sulfur atoms in the dimethyl sulfide molecules adsorbed on three-fold hollow sites, and green dots are the position of the sulfur atoms adsorbed on atop sites.

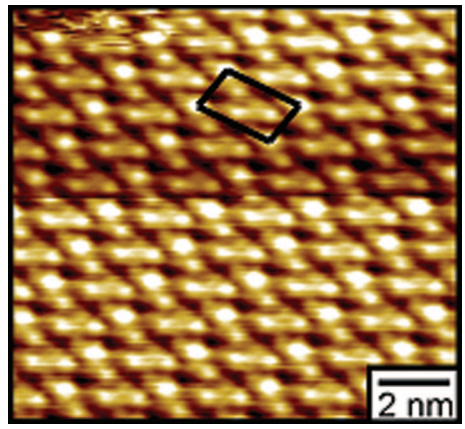

Figure 6. STM image of 0.3 ML (0.36 L) of dimethyl sulfide on Cu{111} at 78 K. This tip state reveals that there are two nonequivalent adsorption sites on the surface. Half the molecules are adsorbed on a site that makes them appear topographically higher than the others. The unit cell is marked in black and has a molecule that images higher than the other molecules at each vertex and a molecule that images lower in its center. Image conditions: $V_{tip} = -0.05$ V, $I = 3.5$ nA.

light blue circles in the model represent the atoms of the underlying Cu{111} terrace. The dark blue circles represent the position of the sulfur atom in the dimethyl sulfide molecules oriented vertically in Figure 5A, and the green circles represent the position of the sulfur atom in the dimethyl sulfide molecules oriented horizontally. The sulfur atoms represented by blue dots are adsorbed in three-fold hollow sites, while those represented by green dots are on atop sites. The two different sulfur adsorption sites account for the slight differences in the appearance of the dimethyl sulfide molecules in Figure 3B that were discussed previously. Experimentally, it was found that side a is 0.70 $\pm$ 0.05 nm and side b is 0.65 $\pm$ 0.05 nm, which is in reasonable agreement with the model in which $a = b = 0.68$ nm. The unit cell in Figure 5A is rotated 17 $\pm$ 5° with respect to the atomic row direction, in agreement with the 19.1° predicted by the model.

The two-adsorption-site model in Figure 5B is further supported by Figure 6, because the unusual tip state in Figure 6 images the dimethyl sulfide molecules with two different topographic heights. This reflects how the nature of a molecule's adsorption site affects its electronic structure, and hence its appearance in the STM image.[37] The same unit cell as shown in Figures 3–5 is seen in Figure 6. The tip state used in Figure 6 imaged the four molecules positioned at the edge of the unit cell topographically higher than the molecule near the center of the unit cell. These observations support our proposed model, in which half the dimethyl sulfide molecules adsorb with their sulfur atoms positioned in a three-fold hollow, while the other half of the molecules adsorb on atop sites.

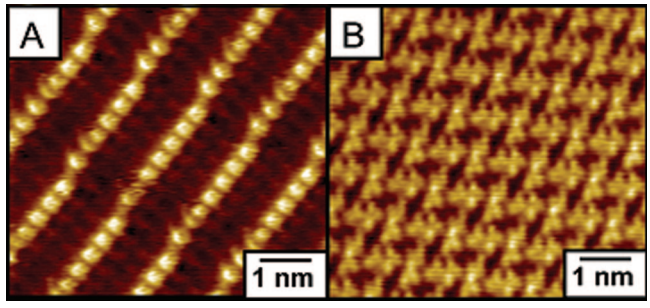

Figure 7. Effect of thioether side-chain length on packing structure. (A) Molecular resolution of dibutyl sulfide on Cu{111} packing in linear chains at 78 K. Each bright spot is the location of the sulfur atom within each molecule. Image conditions: $V_{tip} = -0.01$ V, $I = 10$ pA. (B) Molecular resolution of dimethyl sulfide on Cu{111} at 78 K. Molecules pack in a herringbone arrangement. Image conditions: $V_{tip} = -0.05$ V, $I = 1$ nA.

Dibutyl sulfide has already been studied, and although it is very chemically similar to dimethyl sulfide, it self-organizes in a considerably different arrangement, as shown in Figure 7A.[30] Instead of packing in a herringbone arrangement as dimethyl sulfide does (Figure 7B), dibutyl sulfide packs in linear rows of six or seven molecules before the row is offset half the diameter of a substrate Cu atom to relieve strain.[30] The protrusions correspond to the position of the sulfur atom within the dibutyl sulfide molecule, and the depressed regions on either side of the sulfur atoms are the hydrocarbon chains. The difference in packing structure of the two molecules is due to the competition between intermolecular quadrupole−quadrupole and van der Waals interactions. Dimethyl sulfide has short alkyl chains; therefore, quadrupole−quadrupole interactions dominate the packing energetics and create a herringbone packing structure. Dibutyl sulfide, however, has larger alkyl chains that have increased van der Waals interactions that overpower the quadrupole−quadrupole energy and force the molecules to arrange in linear chains that maximize these interactions. It is important to note that dimethyl sulfide is mobile enough at 78 K to move and form islands, while dibutyl sulfide requires warming to form the long-range order. This difference in mobility at 78 K could explain the difference in island size between the two molecules. At 78 K, dibutyl sulfide formed small islands consisting of only 10–20 molecules, whereas dimethyl sulfide formed much larger islands containing many thousands of molecules.

CONCLUSIONS

By studying the adsorption of dimethyl sulfide on Cu{111} and contrasting the data to those obtained with a larger thioether, dibutyl sulfide, we have revealed some important characteristics about thioether self-assembly: Dimethyl sulfide adsorbs intact at 78 K.At low surface coverage (<0.1 ML), dimethyl sulfide freely diffuses over the surface and preferentially adsorbs at the top of step edges and at single atom defects at 78 K.At higher coverages, dimethyl sulfide packs in regular islands in a herringbone arrangement that maximizes quadrupole−quadrupole interactions. This is in con-

trast to dibutyl sulfide, which forms linear chains on Cu{111} at 78 K driven by van der Waals interactions between the alkyl chains.The packing structure of dimethyl sulfide on Cu{111} has a ($\sqrt{7} \times \sqrt{7}$)R19.1° unit cell in which half the molecules are adsorbed on atop sites and half are adsorbed on three-fold hollow sites.Ordered overlayers of dimethyl sulfide extend over large areas and are mostly free of defects.

When these data are compared to our earlier work on dibutyl sulfide, it is evident that short-chained thioethers form well-ordered SAMs at 78 K without any of the annealing procedures required for dibutyl sulfide. Dimethyl sulfide forms SAMs that are free of the etch pits associated with thiol-based SAMs while being more resistant to oxidation than its thiol counterpart, methanethiol. We demonstrate the effect of changing the length of the alkyl side chains of thioethers on the packing structure of the SAM. We are now beginning to study the stability of thioether SAMs as a function of temperature and chain length.

METHODS

All experiments were conducted using a low-temperature, ultra-high-vacuum (LT-UHV) scanning tunneling microscope purchased from Omicron.[38,39] The microscope was cooled to 78 K, which minimized thermal drift enough to study the same area of the surface for hours at a time.[30,40,41] A Cu{111} crystal was used as the substrate for these experiments, and it was cleaned by many cycles of argon ion sputtering (1 keV/10 μA) and annealing at 820 K. Dimethyl sulfide (99.9% purity) was purchased from Sigma Aldrich and was purified further by cycles of freeze/pump/thaw before being introduced to the STM chamber using a collimated molecular doser. Each dose was timed, and the flux was monitored using an ion gauge in the STM chamber. All coverages are given in both monolayers (ML), where 1 ML corresponds to 1 dimethyl sulfide molecule per 2.75 Cu atoms, and Langmuirs (L). In our setup, a 1 L dose of dimethyl sulfide corresponds to a surface coverage of 0.83 ML. Due to the fact that dimethyl sulfide forms islands on the surface, any local surface coverage will invariably deviate from the overall coverage.

Acknowledgment is made to the donors of the American Chemical Society Petroleum Research Fund (Grant No. 45256-G5) and the NSF (Grant No. 0717978) for support of this research. A.E.B. thanks the U.S. Department of Education for a GAANN fellowship.

Supporting Information Available: STM image of clean Cu{111} surface at 78 K showing standing waves emanating from defects and atomic resolution of the Cu lattice. This information is available free of charge *via* the Internet at http://pubs.acs.org.

REFERENCES AND NOTES

1 Dameron, A. A.; Hampton, J. R.; Smith, R. K.; Mullen, T. J.; Gillmor, S. D.; Weiss, P. S. Microdisplacement Printing. *Nano Lett.* **2005**, *5*, 1834–1837.
2 Donhauser, Z. J.; Mantooth, B. A.; Kelly, K. F.; Bumm, L. A.; Stapleton, J. J.; Price, D. W., Jr.; Allara, D. L.; Tour, J. M.; Weiss, P. S. Conductance Switching in Single Molecules through Conformational Changes. *Science* **2001**, *292*, 2303–2307.
3 Giancarlo, L. C.; Flynn, G. W. Scanning Tunneling and Atomic Force Microscopy Probes of Self-Assembled, Physisorbed Monolayers: Peeking at the Peaks. *Annu. Rev. Phys. Chem.* **1998**, *49*, 297–336.
4 Giancarlo, L. C.; Flynn, G. W. Raising Flags: Applications of Chemical Marker Groups to Study Self-Assembly, Chirality, and Orientation of Interfacial Films by Scanning Tunneling Microscopy. *Acc. Chem. Res.* **2000**, *33*, 491–501.
5 Love, J. C.; Estroff, L. A.; Kriebel, J. K.; Nuzzo, R. G.; Whitesides, G. M. Self-Assembled Monolayers of Thiolates on Metals as a form of Nanotechnology. *Chem. Rev.* **2005**, *105*, 1103–1169.
6 Poirier, G. E. Characterization of Organosulfur Molecular Monolayers on Au{111} using Scanning Tunneling Microscopy. *Chem. Rev.* **1997**, *97*, 1117–1128.
7 Poirier, G. E.; Tarlov, M. J. The C(4 × 2) Superlattice of N-Alkanethiol Monolayers Self-Assembled an Au(111). *Langmuir* **1994**, *10*, 2853–2856.
8 Poirier, G. E.; Tarlov, M. J.; Rushmeier, H. E. 2-Dimensional Liquid-Phase and the Px-Root-3-Phase of Alkanethiol Self-Assembled Monolayers on Au(111). *Langmuir* **1994**, *10*, 3383–3386.
9 Smith, R. K.; Lewis, P. A.; Weiss, P. S. Patterning Self-Assembled Monolayers. *Prog. Surf. Sci.* **2004**, *75*, 1–68.
10 Srinivasan, U.; Houston, M. R.; Howe, R. T.; Maboudian, R. Alkyltrichlorosilane-based Self-Assembled Monolayer Films for Stiction Reduction in Silicon Micromachines. *J. Microelectromech. Syst.* **1998**, *7*, 252–260.
11 Stuart, D. A.; Yuen, J. M.; Lyandres, N. S. O.; Yonzon, C. R.; Glucksberg, M. R.; Walsh, J. T.; Van Duyne, R. P. In Vivo Glucose Measurement by Surface-Enhanced Raman Spectroscopy. *Anal. Chem.* **2006**, *78*, 7211–7215.
12 Xia, Y. N.; Whitesides, G. M. Soft Lithography. *Annu. Rev. Mater. Sci.* **1998**, *28*, 153–184.
13 Qu, H. W.; Yao, W.; Garcia, T.; Zhang, J. D.; Sorokin, A. V.; Ducharme, S.; Dowben, P. A.; Fridkin, V. M. Nanoscale Polarization Manipulation and Conductance Switching in Ultrathin Films of a Ferroelectric Copolymer. *Appl. Phys. Lett.* **2003**, *82*, 4322–4324.
14 Ulman, A. Formation and Structure of Self-Assembled Monolayers. *Chem. Rev.* **1996**, *96*, 1533–1554.
15 Ford, J. F.; Vickers, T. J.; Mann, C. K.; Schlenoff, J. B. Polymerization of a Thiol-Bound Styrene Monolayer. *Langmuir* **1996**, *12*, 1944–1946.
16 Cometto, F. P.; Paredes-Olivera, P.; Macagno, V. A.; Patrito, E. M. Density Functional Theory Study of the Adsorption of Alkanethiols on Cu(111), Ag(111), and Au(111) in the Low and High Coverage Regimes. *J. Phys. Chem. B* **2005**, *109*, 21737–21748.
17 Driver, S. M.; Woodruff, D. P. Adsorption Structures of 1-Octanethiol on Cu(111) Studied by Scanning Tunneling Microscopy. *Langmuir* **2000**, *16*, 6693–6700.
18 Ferral, A.; Paredes-Olivera, P.; Macagno, V. A.; Patrito, E. M. Chemisorption and Physisorption of Alkanethiols on Cu(111). A Quantum Mechanical Investigation. *Surf. Sci.* **2003**, *525*, 85–99.
19 Ferral, A.; Patrito, E. M.; Paredes-Olivera, P. Structure and Bonding of Alkanethiols on Cu(111) and Cu(100). *J. Phys. Chem. B* **2006**, *110*, 17050–17062.
20 Parkinson, G. S.; Munoz-Marquez, M. A.; Quinn, P. D.; Gladys, M. J.; Woodruff, D. P.; Bailey, P.; Noakes, T. C. Q. The Methanethiolate-Induced Pseudo-(100) Reconstruction of Cu(111): A Medium Energy Ion Scattering Structure Study. *Surf. Sci.* **2005**, *598*, 209–217.
21 Driver, S. M.; Woodruff, D. P. Scanning Tunnelling Microscopy Study of the Interaction of Dimethyl Disulphide with Cu(111). *Surf. Sci.* **2000**, *457*, 11–23.
22 Bain, C. D.; Biebuyck, H. A.; Whitesides, G. M. Comparison of Self-Assembled Monolayers on Gold−Coadsorption of Thiols and Disulfides. *Langmuir* **1989**, *5*, 723–727.
23 Noh, J.; Jeong, Y.; Ito, E.; Hara, M. Formation and Domain Structure of Self-Assembled Monolayers by Adsorption of Tetrahydrothiophene on Au(111). *J. Phys. Chem. C* **2007**, *111*, 2691–2695.
24 Noh, J.; Kato, H. S.; Kawai, M.; Hara, M. Surface and Adsorption Structures of Dialkyl Sulfide Self-Assembled

Monolayers on Au(111). *J. Phys. Chem. B* **2002**, *106*, 13268–13272.
25 Noh, J.; Murase, T.; Nakajima, K.; Lee, H.; Hara, M. Nanoscopic Investigation of the Self-Assembly Processes of Dialkyl Disulfides and Dialkyl Sulfides on Au(111). *J. Phys. Chem. B* **2000**, *104*, 7411–7416.
26 Troughton, E. B.; Bain, C. D.; Whitesides, G. M.; Nuzzo, R. G.; Allara, D. L.; Porter, M. D. Monolayer Films Prepared by the Spontaneous Self-Assembly of Symmetrical and Unsymmetrical Dialkyl Sulfides from Solution onto Gold Substrates−Structure, Properties, and Reactivity of Constituent Functional-Groups. *Langmuir* **1988**, *4*, 365–385.
27 Weidner, T.; Kramer, A.; Bruhn, C.; Zharnikov, M.; Shaporenko, A.; Siemeling, U.; Trager, F. Novel Tripod Ligands for Prickly Self-Assembled Monolayers. *Dalton Trans.* **2006**, *23*, 2767–2777.
28 Padowitz, D. F.; Messmore, B. W. STM Observations of Exchange Dynamics at the Solid-Liquid Interface using a Molecular Tracer. *J. Phys. Chem. B* **2000**, *104*, 9943–9946.
29 Padowitz, D. F.; Sada, D. M.; Kemer, E. L.; Dougan, M. L.; Xue, W. A. Molecular Tracer Dynamics in Crystalline Organic Films at the Solid-Liquid Interface. *J. Phys. Chem. B* **2002**, *106*, 593–598.
30 Jensen, S. C.; Baber, A. E.; Tierney, H. L.; Sykes, E. C. H. Adsorption, Interaction and Manipulation of Dibutyl Sulfide on Cu{111}. *ACS Nano* **2007**, *1*, 22–29.
31 Smoluchowski, R. Anisotropy of the Electronic Work Function of Metals. *Phys. Rev.* **1941**, *60*, 661–674.
32 Crommie, M. F.; Lutz, C. P.; Eigler, D. M. Imaging Standing Waves in a 2-Dimensional Electron Gas. *Nature* **1993**, *363*, 524–527.
33 Kamna, M. M.; Stranick, S. J.; Weiss, P. S. Imaging Substrate-Mediated Interactions. *Isr. J. Chem.* **1996**, *36*, 59–62.
34 Stranick, S. J.; Kamna, M. M.; Weiss, P. S. Atomic-Scale Dynamics of a Two-Dimensional Gas-Solid Interface. *Science* **1994**, *266*, 99–102.
35 Terlain, A.; Larher, Y.; Angerand, F.; Parette, G.; Lauter, H.; Bassignana, I. C. Neutron-Diffraction Study of the Structure of the Crystal Monolayer of C2N2 Adsorbed on Graphite(0001). *Mol. Phys.* **1986**, *58*, 799–813.
36 Han, P.; Sykes, E. C. H.; Pearl, T. P.; Weiss, P. S. A Comparative Scanning Tunneling Microscopy Study of Physisorbed linear Quadrupolar Molecules: C2N2 and CS2 on Au{111} at 4 K. *J. Phys. Chem. A* **2003**, *107*, 8124–8129.
37 Weiss, P. S.; Eigler, D. M. Site Dependence of the Apparent Shape of a Molecule in Scanning Tunneling Microscope Images−Benzene on Pt(111). *Phys. Rev. Lett.* **1993**, *71*, 3139–3142.
38 Backer, T.; Hovel, H.; Tschudy, M.; Reihl, B. Applications with a New Low-Temperature UHV STM at 5 K. *Appl. Phys. A: Mater. Sci. Process.* **1998**, *66*, S27–S30.
39 Binnig, G.; Rohrer, H.; Gerber, C.; Weibel, E. 7 × 7 Reconstruction on Si(111) Resolved in Real Space. *Phys. Rev. Lett.* **1983**, *50*, 120–123.
40 Baber, A. E.; Jensen, S. C.; Iski, E. V.; Sykes, E. C. H. Extraordinary Atomic Mobility of Au{111} at 80 Kelvin: Effect of Styrene Adsorption. *J. Am. Chem. Soc.* **2006**, *128*, 15384–15385.
41 Baber, A. E.; Jensen, S. C.; Sykes, E. C. H. Dipole-Driven Ferroelectric Assembly of Styrene on Au{111}. *J. Am. Chem. Soc.* **2007**, *129*, 6368–6369.